Brazilian Journal of Poultry Science
Revista Brasileira de Ciência Avícola

e-ISSN: 1806-9061 2025 / v.27 / n.3 / 001-014

http://dx.doi.org/10.1590/1806-9061-2025-2134

Original Article

Effect of Antimicrobial Peptide Q4-15-2A7P on Growth Performance, Gut Morphology, Intestinal Gene Expression, and Ileal Microbiota in Broilers Challenged with Clostridium perfringens Toxin

■Author(s)

Horng YB[I] https://orcid.org/0009-0007-6503-0015
Cheng YH[I] https://orcid.org/0000-0001-6009-6006
Yu YH[I] https://orcid.org/0000-0001-9629-8478
Chen WJ[I] https://orcid.org/0000-0001-7489-1019

[I] National Ilan University, Department of Biotechnology and Animal Science, Yilan, Taiwan.

■Mail Address

Corresponding author e-mail address
Wei-Jung Chen
National Ilan University, Department of Biotechnology and Animal Science, No.1, Sec. 1, Shennong Rd., Yilan City, Yilan County 26047, Taiwan.
Phone: +886 3 931 7623
Email: wjchen@niu.edu.tw

■Keywords

Antimicrobial peptide, broiler, *Clostridium perfringens*, growth, phospholipase C.

Section Editor: Irenilza de Alencar Nääs

Submitted: 29/June/2025
Approved: 06/August/2025

ABSTRACT

This study investigated the effects of antimicrobial peptide Q4-15-2A7P on the growth performance and gut health of broilers under *Clostridium perfringens* toxin challenge. A total of 144 one-day-old broiler chicks (Ross 308) were assigned to four groups: negative control (NC), positive control (PC; phospholipase C [PLC, *C. perfringens* toxin] challenge), prevention peptide group (PP; PLC challenge + 20 mg/kg Q4-15-2A7P from days 1–35), and therapy peptide group (TP; PLC challenge + 20 mg/kg Q4-15-2A7P from days 23–35). PLC (150 U/mL) was orally administered from days 19 to 21. Results showed that feed intake in the PP group from days 1 to 27 recovered to NC levels, whereas the PC group exhibited severe intestinal lesions. At 35 days, ileal lesion scores in the PP and TP groups were comparable to those of healthy birds. At 28 days, PP and TP groups had lower expression of inflammation-associated genes in the ileum, and the PP group showed increased expression of tight junction genes. The expression of tight junction-associated genes in the ileum were not induced in the TP group at 28 days, as opposed to the PP group. The microbiota in the PP and TP groups closely resembled that of the NC group. In conclusion, both preventive and therapeutic peptide strategies effectively mitigated PLC-induced pathology, with the PP group showing the most pronounced gut health improvement.

INTRODUCTION

The poultry industry has historically depended on antibiotic growth promoters (AGPs) to enhance production efficiency. However, the rise of antimicrobial resistance (AMR) has become a serious concern, prompting the World Health Organization to label AMR as a global epidemic and highlighting the urgent need for effective AGP alternatives. *Clostridium perfringens*, a major pathogen in poultry, is the primary causative agent of necrotizing enteritis (NE), a disease that causes an annual economic loss estimated at US$2–6 billion for the industry (Fathima *et al.*, 2022). Moreover, the increasing prevalence of multidrug-resistant (MDR) bacterial strains in poultry further complicates treatment strategies and diminishes the efficacy of conventional antibiotics. As AGP usage continues to decline globally, developing alternative strategies for controlling NE and other bacterial infections has become imperative.

Recent investigations have underscored the potential of antimicrobial peptides (AMPs) as viable alternatives to conventional antibiotics for controlling *C. perfringens* infections in livestock. AMP derived from *Bombyx mandarina* exhibits potent antimicrobial activity against *C. perfringens* (Liang *et al.*, 2022). It has been demonstrated that inoculation of a plasmid encoding chicken interleukin-17 upregulated the expression of β-defensin and cathelicidin in the gut, thereby reducing NE lesions in broilers under *C. perfringens* challenge (Boodhoo

et al., 2024). Moreover, supplementation with AMP effectively reduced the numbers of *C. perfringens* in the lower jejunum of broilers without adversely affecting growth performance (Fodor *et al.*, 2023). Collectively, these findings indicate that AMPs can inhibit *C. perfringens* growth *in vitro* and *in vivo*, thereby offering a potential strategy to mitigate NE in poultry. In addition to their direct antimicrobial effects, AMPs also exhibit significant anti-inflammatory properties. One study demonstrated that de novo designed short peptides not only provide broad-spectrum antibacterial activity but also suppress inflammatory responses in macrophages (Son *et al.*, 2022). Another investigation revealed that a helix-to-helix structured peptide inhibits lipopolysaccharide-induced pro-inflammatory cytokine production and alleviates endotoxin-mediated sepsis in mouse models (Kim *et al.*, 2022). Furthermore, branched peptides derived from natural host defense sequences have been shown to both inhibit bacterial growth and modulate inflammatory responses in murine skin infection models (Meogrossi *et al.*, 2024).

A key virulence factor of *C. perfringens* is phospholipase C (PLC), a zinc-dependent enzyme that catalyzes the hydrolysis of membrane phospholipids (Kiu and Hall, 2018). This enzymatic activity disrupts the structural integrity of host cell membranes, leading to cytolysis, the release of intracellular contents, and the generation of reactive oxygen species (ROS), which together contribute to oxidative stress and trigger downstream inflammatory and apoptotic signaling cascades (Kiu & Hall, 2018). A recent *in vitro* study has demonstrated that exposure to PLC results in marked cytotoxicity in Leghorn male hepatoma cells, underscoring its potent membrane-damaging effects (Wang *et al.*, 2024). PLC-induced membrane disruption compromises the intestinal epithelial barrier *in vivo*, facilitating bacterial translocation and eliciting an exacerbated inflammatory response that is central to the pathogenesis of NE. A toxinotyping study further revealed that all virulent *C. perfringens* strains harbor the *plc* gene, confirming the ubiquitous role of alpha toxin in NE, while additional toxins such as NetB and zinc metallopeptidases act synergistically to enhance cytotoxicity (Wade *et al.*, 2020). These findings not only elucidate the multifaceted mechanisms by which PLC inflicts tissue damage and dysregulates host immunity but also highlight its critical contribution to NE pathogenesis.

Our research team has developed a series of custom cationic peptides, such as GW-Q4 (GANAAKKFATIAKKFINYLW). GW-Q4 was then modified based on systematic modulation of four key structural parameters: charge, hydrophobicity, polar angle, and hydrophobic moment (Chou *et al.*, 2008). The mechanism of these peptides was subsequently validated, confirming that they selectively target and disrupt bacterial-mimicking anionic membranes (Chou *et al.*, 2010). To optimize these peptides for veterinary applications, a truncated GW-Q4 was developed (Q4-15) by reducing the number of amino acid from 20 to 15 and performed strategic substitutions of a key tyrosine residue with lysine (to create Q4-15-1) or tryptophan (Q4-15-2) to enhance antimicrobial efficacy against pathogens. The truncated version of GW-Q4 (named Q4-15) exhibited potent antibacterial activity against multidrug-resistant enterotoxigenic *Escherichia coli*—and inhibit biofilm formation (Wu *et al.*, 2021). Subsequent modifications through proline substitution within the hydrophobic region, as demonstrated in related peptide studies (Yeaman *et al.*, 2003; Chou *et al.*, 2008), led to the creation of Q4-15-2A7P—a peptide with enhanced membrane-disruptive activity and reduced cytotoxicity—underscoring its significant potential as an antibacterial agent.

We hypothesize that Q4-15-2A7P serves as an effective alternative to antibiotics through two mechanisms. First, Q4-15-2A7P may modulate the gut microbiota of broilers due to its antibacterial activity, fostering an environment less conducive to PLC damage. Furthermore, previous studies have reported that AMPs are able to modulate inflammatory responses (Kim *et al.*, 2022; Son *et al.*, 2022; Meogrossi *et al.*, 2024). Therefore, secondly, Q4-15-2A7P may interfere with PLC-mediated inflammatory response, thereby inhibiting NE progression in broilers. These mechanisms render Q4-15-2A7P a promising alternative to antibiotics, potentially offering a novel approach to poultry disease management through both preventive and therapeutic applications, addressing the growing challenge of antimicrobial resistance.

MATERIALS AND METHODS

Ethics statement

The protocol of the animal experiment was reviewed and approved by the Institutional Animal Care and Use Committee of National Ilan University (112-10).

Design and synthesis of AMPs

The peptide used in this study, Q4-1ana-2-A7P, is a rationally designed derivative from a series developed in our previous work. This series originated from the parent peptide GW-Q4 (GANAAKKFATIAKKFINYLW), which was initially designed and synthesized based

on four key structural parameters (charge, polar angle, hydrophobicity, and hydrophobic moment) to achieve high antimicrobial activity and selectivity. Its mechanism of selectively targeting and disrupting anionic membranes that mimic bacterial cell walls was subsequently validated. For applications against livestock pathogens, GW-Q4 was truncated to a shorter 15-amino-acid version, Q4-15 (KKFATIAKKFINYLW), to create a more cost-effective yet potent molecule. To further enhance its bioactivity, a key tyrosine (Y) residue in Q4-15 was substituted with tryptophan (W) to yield Q4-15-2 (KKFATIAKKFINWLW). The purpose of this substitution was to increase the peptide's overall hydrophobicity, a critical property for improving its ability to disrupt bacterial cell membranes. For the present study, a final modification was made to Q4-15-2. A proline residue was substituted into the hydrophobic face to create the final peptide, Q4-15-2A7P (Figure 1). This was done to introduce a structural kink intended to enhance selective cytotoxicity against bacterial cells while minimizing non-specific toxicity towards host cells. The final Q4-15-2A7P peptide was synthesized by Kelowna International Scientific (New Taipei City, Taiwan). Its chemical formula is C98H147N23O17, and its molecular weight is 1919.35 Da.

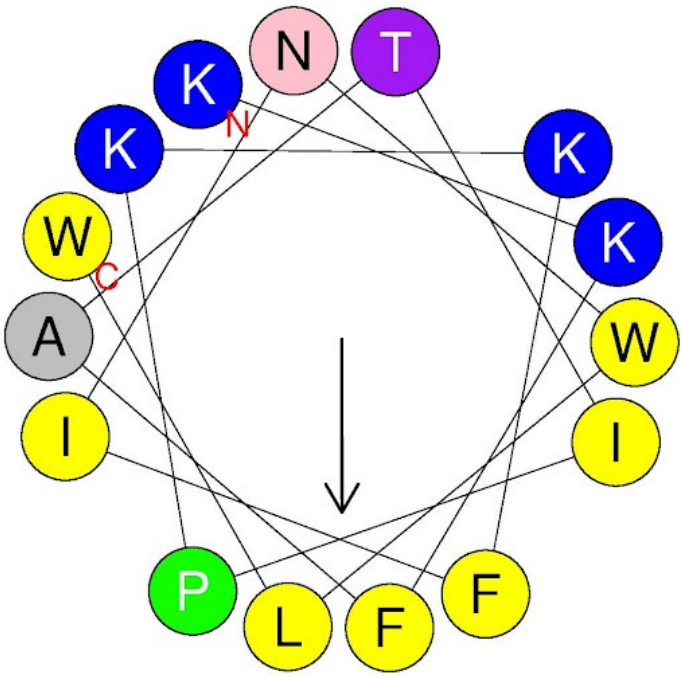

Figure 1 – Helical wheel projection of AMPs Q4-15-2 A7P (KKFATIPKKFINWLW), drawn on HeliQuest (https://heliquest.ipmc.cnrs.fr/index.html).

Bacterial culture, and extraction of phospholipase C

C. perfringens (ATCC 13124) was obtained from the Food Industry Research and Development Institute (Hsinchu, Taiwan). The bacterium was first revived from frozen stock on blood agar plates under strict anaerobic conditions at 37 °C for 24 h. A single, well-isolated colony was then inoculated into 50 mL of pre-reduced reinforced *Clostridium* medium (RCM) in an anaerobic chamber, using a 4% (v/v) inoculum. Cultures were incubated at 37 °C for an additional 24 h with gentle agitation (approximately 100 rpm) until the bacterial count exceeded 10^9 CFU/mL, as determined by optical density measurement at 600 nm and confirmed by serial dilution plating. For PLC extraction, the entire 24-h culture was transferred to 250-mL centrifuge bottles and centrifuged at 6000 rpm for 15 min at 4 °C to pellet the bacterial cells. The supernatant, which contains the secreted PLC, was decanted carefully and further clarified by filtration through a 0.22 µm membrane filter to remove any residual cells. To concentrate the enzyme, the filtrate was subjected to ammonium sulfate precipitation at 70% saturation with continuous stirring at 4 °C for 2 h. The precipitated proteins were recovered by centrifugation at 10,000 rpm for 20 min, resuspended in 10 mM Tris-HCl buffer (pH 7.4), and dialyzed overnight at 4 °C against the same buffer. The dialysate, now enriched in PLC, was further purified using ion exchange chromatography (DEAE-Sepharose) followed by gel filtration chromatography (Sephadex G-75). The enzymatic activity was determined using a standard egg yolk lecithin assay, and the final PLC preparation was adjusted to a concentration of 150 U/mL for use in subsequent experiments. The supernatant containing PLC was collected, and its content was quantified using commercial PLC standards (Möllby *et al.*, 1973; Fatmawati *et al.*, 2013). Specifically, PLC from *C. perfringens* (Type I, lyophilized powder, 10–50 units/mg protein, CAS No. 9001-86-9) was purchased from Sigma-Aldrich (St. Louis, MO, USA; Cat. No. P7633). This product contained 45.5 mg of solid (711 units/mg solid; 31 mg protein) and was stored at –20 °C according to the manufacturer's instructions. The concentration of PLC was then adjusted to 150 U/mL for experimental use, and the solution was stored at –80 °C until needed.

Experimental design of the animal study

A total of 144 one-day-old, unsexed Ross-308 broilers, with an average initial body weight of 45 ± 1.4 g, were used in this experiment. The broilers were randomly assigned to one of four treatment groups, with 6 replicates of 4 broilers per cage, following a completely randomized design. The experimental diets were as follows: (1) a basal diet with no treatment

(negative control, NC), (2) a basal diet plus *C. perfringens* toxin challenge (150 U PLC/day, positive control, PC), (3) a basal diet plus *C. perfringens* toxin challenge (150 U PLC/day) and 20 mg/kg of Q4-15-2A7P from day 1 to 35 (prevention peptide, PP), and (4) a basal diet plus *C. perfringens* toxin challenge (150 U PLC/day) and 20 mg/kg of Q4-15-2A7P from days 21 to 35 (therapy peptide, TP). A 1-mL aliquot of *C. perfringens* toxin solution (150 U PLC) was orally administered to the broilers from days 19 to 21. The concentration of Q4-15-2A7P in the diet of broiler is based on a previous study (Wang *et al.*, 2016). The experimental diets (Table 1) were formulated in accordance with the nutrient specifications outlined in the Aviagen 2022 Broiler Nutrition Specifications. Nutrient levels were adjusted based on the target live weight categories and corresponding growth phases for Ross broilers, ensuring that the diets provided energy, digestible amino acids, minerals, and vitamins within the recommended ranges to support optimal performance and carcass yield.

Table 1 – Basal diet composition.

Item	Starter (1-10d)	Grower (11-24d)	Finisher (25-35d)
Ingredient (%)			
Corn, yellow	55.0	57.0	62.0
Soybean meal 44.0 % CP	30.0	30.0	27.5
Fish meal	5.0	5.0	3.5
Limestone, 38 %	2.0	1.5	1.3
Dicalcium phosphate	1.0	0.8	0.7
Salt	0.4	0.4	0.4
Choline, 60 %	0.02	0.02	0.02
Vitamin and mineral mix[1]	0.10	0.10	0.10
Methionine 99.5 %	0.20	0.18	0.16
Calculated nutritional contents (%)			
Crude protein %	23.0	21.5	19.5
ME, kcal/kg	2975	3050	3100
Fat %	3.47	3.24	3.26
Fiber %	4.24	3.42	3.36
Ca %	0.95	0.75	0.65
P %	0.50	0.42	0.36
Lysine %	1.32	1.18	1.08
Methionine+ Cystine %	1.00	0.92	0.86
Moisture %	12.45	11.24	11.38

[1]Supplied per kilogram of diet: 1.8 mg of all-trans-retinyl acetate, 0.02 mg of cholecalciferol, 8.3 mg of alpha-tocopheryl acetate, 2.2 mg of menadione, 2 mg of pyridoxine HCl, 8 mg of cyanocobalamin, 10 mg of nicotinamide, 0.3 mg of folic acid, 20 mg of D-biotin, and 160 mg of choline chloride.
[2]Supplied per kilogram of diet: 32 mg of manganese ($MnSO_4 \cdot H_2O$), 16 mg of iron ($FeSO_4 \cdot 7H_2O$), 24 mg of zinc (ZnO), 2 mg of copper ($CuSO_4 \cdot 5H_2O$), 800 mg of iodine (KI), 200 mg of cobalt ($CoSO_4$), and 60 mg of selenium.

The experiment lasted 35 days. All broilers were housed in cages (1 m × 0.8 m × 0.8 m) with slatted plastic floors. The room temperature was initially set at 30 °C and gradually reduced to 24 °C by the end of the study. The lighting schedule consisted of 18 h of light and 6 h of darkness (18L:6D) throughout the experiment. Food and water were provided ad libitum. Individual body weight, average daily feed intake, average daily weight gain, and feed conversion ratio were recorded weekly.

Tissue collection and analysis

At 28 and 35 days of age, 2 birds per replicate were randomly selected and euthanized through carbon dioxide inhalation. Four replicates (n=4) were used for intestinal lesion scoring and gut morphology analysis. Intestinal lesions were scored using a standardized index method, based on specific lesion indicators such as inflammation and necrosis. A total lesion score was calculated by assessing multiple lesion parameters. Intestinal segments were fixed in 10% phosphate-buffered formalin, stained with hematoxylin and eosin, and examined under a microscope. Intestinal damage was then determined and compared between groups, with a scoring system as follows: 1 = 1%–25%, 2 = 26%–50%, 3 = 51%–75%, and 4 = 76%–100%, with red dots indicating tissue damage (Rautenschlein *et al.*, 2005). A lower score indicated better health, whereas a higher score indicated more severe and obvious lesions. At the time of slaughter, the inner wall patterns of 3 intestinal sections were exposed and immediately photographed. Samples from the duodenum, jejunum, and ileum were collected, soaked, and fixed in formalin for 2 weeks. After fixation, these sections were cut into appropriate sizes, dehydrated using a dehydrator for 12 h, paraffin-embedded, sectioned, and stained. The villus length and crypt depth of the different intestinal segments were measured and analyzed.

RNA extraction, cDNA synthesis, and quantitative reverse-transcription PCR

At 28 and 35 days of age, ileal tissue from 2 broilers per replicate was freshly collected and pooled. Three replicates (n=3) were used for ileal gene expression analysis. Total RNA was extracted from ileum by using TRIzol Reagent (Invitrogen, CA, USA). cDNA was synthesized from these RNA templates by using a Transcriptor Reverse Transcriptase kit (Roche Applied Science, IN, USA). mRNA levels in the ileum were quantified through qPCR by using the Miniopticon Real-Time PCR Detection System (Bio-Rad, CA, USA) and the KAPA SYBR FAST qPCR Kit (Kapa Biosystems, Inc., MA, USA). The primer sequences used in this study are presented in Table 2. The qPCR conditions were as follows: an initial denaturation at 95°C for 2

min, followed by 40 cycles of 95°C for 15 s and 55°C for 15 s. Relative mRNA expression levels for each gene were normalized to β-actin and analyzed using the $2^{-\Delta\Delta Ct}$ method.

Table 2 – Sequences of the primers used in the quantitative RT-PCR.

Gene	Sequence (5'-3')	Accession number
IL-1β	F: CGCTCACAGTCCTTCGAC R: TGAGCCTCACTTTCTGGC	NM_204524.2
IL-6	F: AGGACGAGATGTGCAAGAAGTTC R: TTGGGCAGGTTGAGGTTGTT	NM_204628.2
TNF-α	F: GAGCGTTGACTTGGCTGTC R: AAGCAACAACCAGCTATGCAC	AY765397.1
JAM-2	F: AATTTACAGTTCCTCCCACT R: GTCTTTTCCAGTAAGGCAAC	NM_001006257
ZO-1	F: CACACTGTGACCCCAAAA R: AAGGTCCATCTCAGTTTCAC	XM_040680632
OCLN	F: TCGTGCTGTGCATCGCCATC R: CGCTGGTTCACCCCTCCGTA	NM_205128
CLDN	F: GGTATGGCAACAGAGTGGCT R: CAGCCAATGAAGAGGGCTGA	NM_001013611.2
β-actin	F: CACCCACACCCCTGTGATGA R: AGAACTTTGGGGGCGTTCGC	NM_205518.1

Abbreviations: IL-1β, interleukin 1β; IL-6, interleukin 6; TNF-α, tumor necrosis factor-α, JAM-2, junctional adhesion molecule 2; ZO-1, zonula occludens-1; OCLN, occludin; CLDN, claudin.

16S rRNA gene sequencing

At 35 days of age, ileal digesta from 2 broilers per replicate were freshly collected and pooled. Three replicates (n = 3) were used for ileal microbiota analysis among the four experimental groups (NC, PC, PP, TP). Total genomic DNA from the ileal digesta was extracted using a commercial DNA extraction kit (D4300, Zymo Research, Irvine, CA, USA). DNA concentration and purity were assessed using spectrophotometry and agarose gel electrophoresis. DNA amplicons were generated from individual broiler samples by using specific primers targeting the V3-V4 regions of the 16S rRNA gene through PCR. The PCR products were then purified using a commercial DNA purification kit (QIAGEN, Germantown, MD, USA), and sequencing libraries were constructed using TruSeq Nano DNA Library Prep Kits (Illumina, San Diego, CA, USA). Library quality was assessed using a Qubit 2.0 Fluorometer (Thermo Scientific, Waltham, MA, USA) and an Agilent Bioanalyzer 2100 system. Sequencing was performed on an Illumina MiSeq platform, generating an average read length of 300 bp. Sequences were clustered into operational taxonomic units (OTUs) at 97% identity by using a clustering program. Alpha and beta diversity analyses were conducted using QIIME 2 (version 2017.4) software and the Ribosomal Database Project classifier Bayesian Algorithm (http://rdp.cme.msu.edu/), respectively. Alpha diversity was assessed using species richness estimators (Chao1 and Fisher alpha) and species evenness estimators (Shannon and Enspie) across the four groups. Beta diversity was evaluated through principal component analysis (PCA) and principal coordinate analysis (PCoA) based on UniFrac distance matrices for the four groups. Similarities and differences in OTUs between the four groups were visualized using a Venn diagram (version 1.6.17).

Statistical analysis

Individual cages were considered replicates, and each replicate was defined as an experimental unit. All data were analyzed using SAS software (version 9.4, 2012; SAS Institute, Cary, NC, USA). The data were tested for normality by using the Shapiro–Wilk test and homogeneity of variance test by using the Levene's test. One-way analysis of variance followed by Tukey's honestly significant difference test was used for analyzing differences. A p value of < 0.05 indicated statistical significance.

RESULTS

PLC extraction and activity determination

For the culture, extraction, and quantification of PLC from cultured bacterial liquid, yolk activity zone results were used to compare the PLC standard with the separated supernatant. The PLC standard curves were used to determine the concentration of PLC from cultured bacterial liquid, and the activity results are presented in Table 3. As shown in Figure 2, the measurements for C1, with 2 repetitions, were 2.54 and 2.56 cm, and those for C2 were 2.39 and 2.42 cm. The PLC activities for C1 and C2 were 6.25 and 4.68 U/mL, respectively. In pre-animal testing, PLC was used to challenge white broilers at low (100 U/mL), medium (150 U/mL), and high (200 U/mL) concentrations at 19 to 21 days of age. After 3 consecutive days of challenge, the results were analyzed, and the 150 U/mL dose was demonstrated to most closely mimic the effects of a challenge with *C. perfringens* (Cheng *et al.*, 2018).

Table 3 – Activity of phospholipase C isolated from *C. perfringens*.

Sample No.	C1-1[1]	C1-2	C2-1	C2-2
Zone (cm)[2]	2.54	2.56	2.39	2.42
Average activity (U/mL)[3]	6.52		4.68	

[1] C1-1 and C2-2 are extract samples obtained from the supernatant of *C. perfringens* cultures, with each sample prepared in duplicate.
[2] The effective diameter is measured using a ruler, and the discolored area caused by PLC is measured.
[3] The average activity was calculated using the average of 2 replicates of the sample.

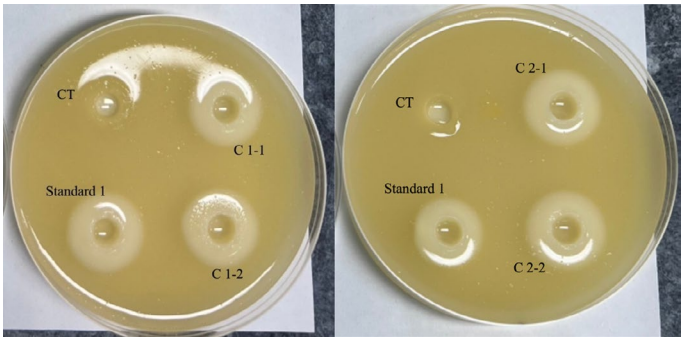

Figure 2 – Discoloration zone formed through phospholipase C hydrolysis of 5% egg yolk lecithin in Columbia agar. Abbreviations: CT, control; C1-1 to C2-2, cultured *C. perfringens* liquid sample replicate. Commercial phospholipase C was used as standard.

Effect of Q4-15-2A7P on growth performance and intestinal lesion scores in broilers

The effects of Q4-15-2A7P treatments on broiler growth performance are summarized in Table 4. No significant between-group differences were observed in terms of body weight, average daily gain, or mortality during the experimental period among the NC, PC, PP, and TP groups. However, the PC group had a significantly lower average daily feed intake at 1–27 days of age compared with the NC, PP, and TP groups (p<0.05). Furthermore, the PC group exhibited a decreased feed conversion ratio at 1–27 days of age compared with the NC, PP, and TP groups (p<0.05). The effects of Q4-15-2A7P treatments on intestinal lesion scores are presented in Figure 3 and Table 5. At 28 days of age, the PC group had significantly higher ileal lesion scores compared with the NC group (p<0.001), while the PP and TP groups showed intermediate levels with no significant difference from NC. No significant differences were observed among groups in the duodenum and jejunum. At 35 days of age, the NC group maintained the lowest duodenal lesion score compared with the PC, PP, and TP groups (p<0.001). In the jejunum, the PC group had a significantly higher lesion score compared with the NC and TP groups (p<0.001), while the PP group was intermediate but not significantly different from NC. In the ileum, the NC, PP, and TP groups had significantly lower lesion scores compared with the PC group (p<0.001), indicating effective recovery in the Q4-15-2A7P-treated groups.

Table 4 – Effect of the antimicrobial peptide Q4-15-2A7P on the growth performance of broilers.

	NC[1]	PC	PP	TP	SEM	*p*-value
BW (g/bird)[3]						
1 d	48.0[2]	47.9	48.2	48.1	0.24	0.32
27 d	1295.0	1279.2	1278.3	1291.9	63.69	0.95
35 d	2018.3	1865.0	1965.7	1941.7	163.8	0.46
ADG (g/d/bird)						
1 - 27 d	44.5	44.0	43.9	44.4	2.27	0.95
28 - 35 d	103.3	83.7	98.1	92.8	27.7	0.66
1 - 35 d	56.3	51.9	54.8	54.1	4.68	0.46
ADI (g/d/bird)						
1 - 27 d	65.7[a]	56.5[b]	64.6[a]	66.9[a]	4.29	< 0.05
28 - 35 d	110.4	111.5	112.0	99.0	26.18	0.80
1 - 35 d	74.7	67.5	74.1	73.3	7.68	0.37
FCR						
1 - 27 d	1.5[b]	1.3[a]	1.5[b]	1.5[b]	0.09	< 0.05
28 - 35 d	1.2	1.8	1.2	1.1	0.87	0.45
1 - 35 d	1.3	1.3	1.4	1.3	0.20	0.99
Mortality (%)						
1 - 35 d	0	0	0	0	0	0

[1] NC, basal diet; PC, basal diet plus 150 U PLC/day; PP, basal diet plus 150 U PLC/day and 20 mg/kg peptide Q4-15-2A7P from 1 to 35 days; TP, basal diet plus 150 U PLC/day and 20 mg/kg peptide Q4-15-2A7P from 23 to 35 days. [2] Mean values represent results from 6 replicate cages per treatment (n=6). [3] Abbreviations: BW, body weight; ADG, average daily gain; ADI, average daily feed intake; FCR, feed conversion ratio. [a-b] Mean values in the same row with different superscript letters are significantly different (p<0.05).

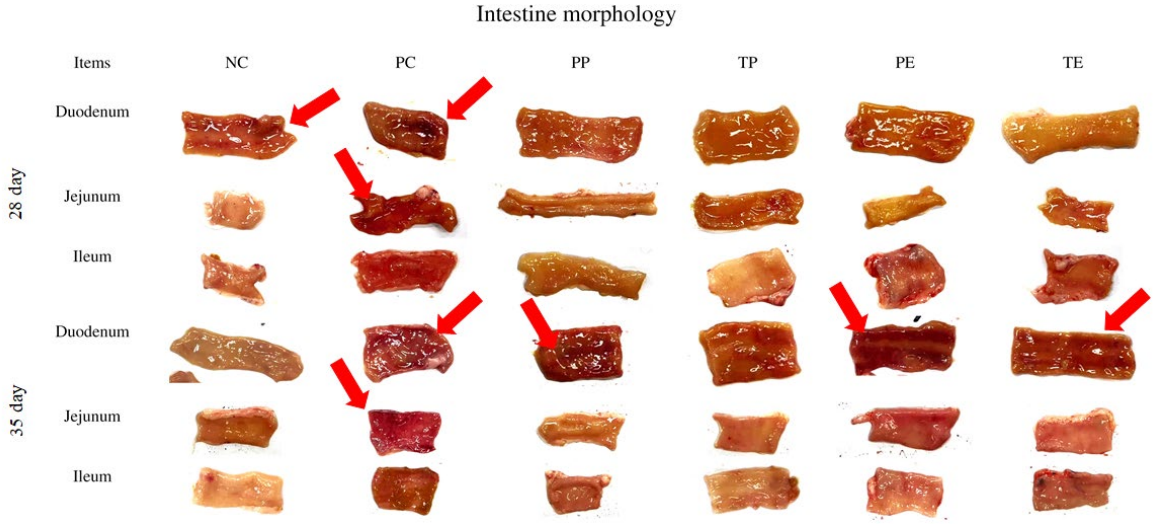

Figure 3 – Gross appearance of small intestines in samples collected at 28 and 35 days of age from four experimental groups: negative control (NC, basal diet), positive control (PC, basal diet + phospholipase C [PLC] challenge), prevention peptide (PP, basal diet + PLC challenge + 20 mg/kg antimicrobial peptide Q4-15-2A7P from days 1 to 35), and therapy peptide (TP, basal diet + PLC challenge + 20 mg/kg antimicrobial peptide Q4-15-2A7P from days 23 to 35). Red arrow indicates intestinal damage. Four replicates were conducted, and one representative replicate is shown (n=4).

Table 5 – Effect of the antimicrobial peptide Q4-15-2A7P on scores for lesions in the small intestine of broilers.

	28 d					
	NC[1]	PC	PP	TP	SEM	*p*-value
Duodenum	1.5[2]	2.7	2.3	2.7	0.95	0.16
Jejunum	1	2.5	1.8	2	1.22	0.24
Ileum	0.3[b]	1.7[a]	0.8[ab]	0.7[ab]	0.63	0.01
	35 d					
	NC[1]	**PC**	**PP**	**TP**	**SEM**	***p*-value**
Duodenum	1.3[b]	3.8[a]	3.3[a]	3.2[a]	0.58	< 0.001
Jejunum	1.0[bc]	3.7[a]	2.2[ab]	0.3[c]	0.99	< 0.001
Ileum	0.2[b]	2.3[a]	0.7[b]	0.7[b]	0.71	< 0.001

[1] NC, basal diet; PC, basal diet plus 150 U PLC/day; PP, basal diet plus 150 U PLC/day and 20 mg/kg peptide Q4-15-2A7P from 1 to 35 days; TP, basal diet plus 150 U PLC/day and 20 mg/kg peptide Q4-15-2A7P from 23 to 35 days.
[2] Mean values represent results from 4 replicate cages per treatment (n=4).
[a-c] Mean values in the row with different superscripted letters are significantly different ($p<0.05$)

Effect of Q4-15-2A7P on gut morphology in broilers

The effects of Q4-15-2A7P treatments on gut morphology in broilers are summarized in Table 6.

Table 6 – Effect of the antimicrobial peptide Q4-15-2A7P on gut morphology in broilers.

		28 d					
		NC[1]	PC	PP	TP	SEM	*p*-value
Duodenum	VH (μm)[3]	1550[2,ab]	1225[b]	1608[a]	1450[ab]	133.1	0.04
	CD (μm)	150[a]	133[ab]	92[ab]	83[b]	2.2	0.03
	VH/CD ratio	10.6	9.8	18.0	17.8	3.59	0.05
Jejunum	VH (μm)	833	675	900	817	147.8	0.37
	CD (μm)	100[ab]	142[a]	100[ab]	67[b]	27.3	0.08
	VH/CD ratio	8.7[ab]	5.1[b]	9.0[ab]	12.6[a]	2.55	0.03
Ileum	VH (μm)	833	700	842	800	57.6	0.07
	CD (μm)	83	100	75	67	19.1	0.08
	VH/CD ratio	11.5	7.2	11.2	16.0	3.2	0.08
		35 d					
		NC[1]	**PC**	**PP**	**TP**	**SEM**	***p*-value**
Duodenum	VH (μm)	1608[a]	1108[b]	1458[a]	1517[a]	120.9	0.01
	CD (μm)	208[a]	125[b]	158[b]	108[ab]	28.6	0.02
	VH/CD ratio	8.2[b]	8.9[b]	12.5[a]	9.7[ab]	1.2	0.01
Jejunum	VH (μm)	783	800	967	900	124.1	0.19
	CD (μm)	100	75	118	142	28.6	0.13
	VH/CD ratio	9.7	10.7	9.6	6.9	3.65	0.64
Ileum	VH (μm)	808	583	708	675	97.1	0.14
	CD (μm)	83	100	83	117	22.4	0.3
	VH/CD ratio	8.2[b]	8.9[b]	12.5[a]	9.7[ab]	1.8	0.02

[1] NC, basal diet; PC, basal diet plus 150 U PLC/day; PP, basal diet plus 150 U PLC/day and 20 mg/kg peptide Q4-15-2A7P from 1 to 35 days; TP, basal diet plus 150 U PLC/day and 20 mg/kg peptide Q4-15-2A7P from 23 to 35 days.
[2] Mean values represent results from 4 replicate cages per treatment (n=4).
[3] Abbreviations: VH, villus height; CD, crypt depth.
[a-b] Mean values in the row with different superscripted letters are significantly different ($p<0.05$)

At 28 days of age, the villus height (VH) in the duodenum in the PP group was significantly greater than that in the PC group ($p=0.04$), while the NC and TP groups showed intermediate values with no significant difference from either. The crypt depth (CD) in the duodenum in the TP group was significantly lower than that in the NC group ($p=0.03$), with the PC and PP groups showing intermediate values. The VH:CD ratio in the jejunum was significantly lower in the PC group compared with the TP group ($p=0.03$), while NC and PP were intermediate. In the ileum, no significant differences were observed in VH, CD, or VH:CD. At 35 days of age, the VH in the duodenum in the NC, PP, and TP groups was significantly higher than that in the PC group ($p=0.01$). The CD in the duodenum in the NC group was significantly higher than that in the PC and PP groups ($p=0.02$), while the TP group was not significantly different from others. The VH:CD ratio in the duodenum and ileum was significantly higher in the PP group compared with the NC and PC groups ($p=0.01$ and $p=0.02$, respectively), with TP showing intermediate values. No significant between-group differences were identified in the jejunum morphology at 35 days.

Effect of Q4-15-2A7P on ileal inflammation and tight-junction protein-associated gene expression in broilers

The effects of Q4-15-2A7P treatments on ileal inflammation-associated gene expression are presented in Figure 4. At 28 days of age, the mRNA levels of IL-1β and IL-6 were significantly higher in the PC group compared with the NC, PP, and TP groups ($p<0.05$). The TNF-α mRNA levels in the PC group were significantly higher than those in the NC, PP, and TP groups ($p<0.05$). At 35 days of age, no significant between-group differences in ileal inflammation-associated gene expression were observed among the four groups. The effects of Q4-15-2A7P treatments on ileal tight-junction protein-associated gene expression are presented in Figure 5. At 28 days of age, the mRNA levels of occludin, ZO-1, claudin, and JAM-2 were significantly higher in the PP group compared with the NC, PC, and TP groups ($p<0.05$). At 35 days of age, occludin, claudin, and JAM-2 mRNA levels were significantly reduced in the PC, PP, and TP groups compared with the NC group ($p<0.05$), while ZO-1 mRNA levels showed no significant differences among the groups.

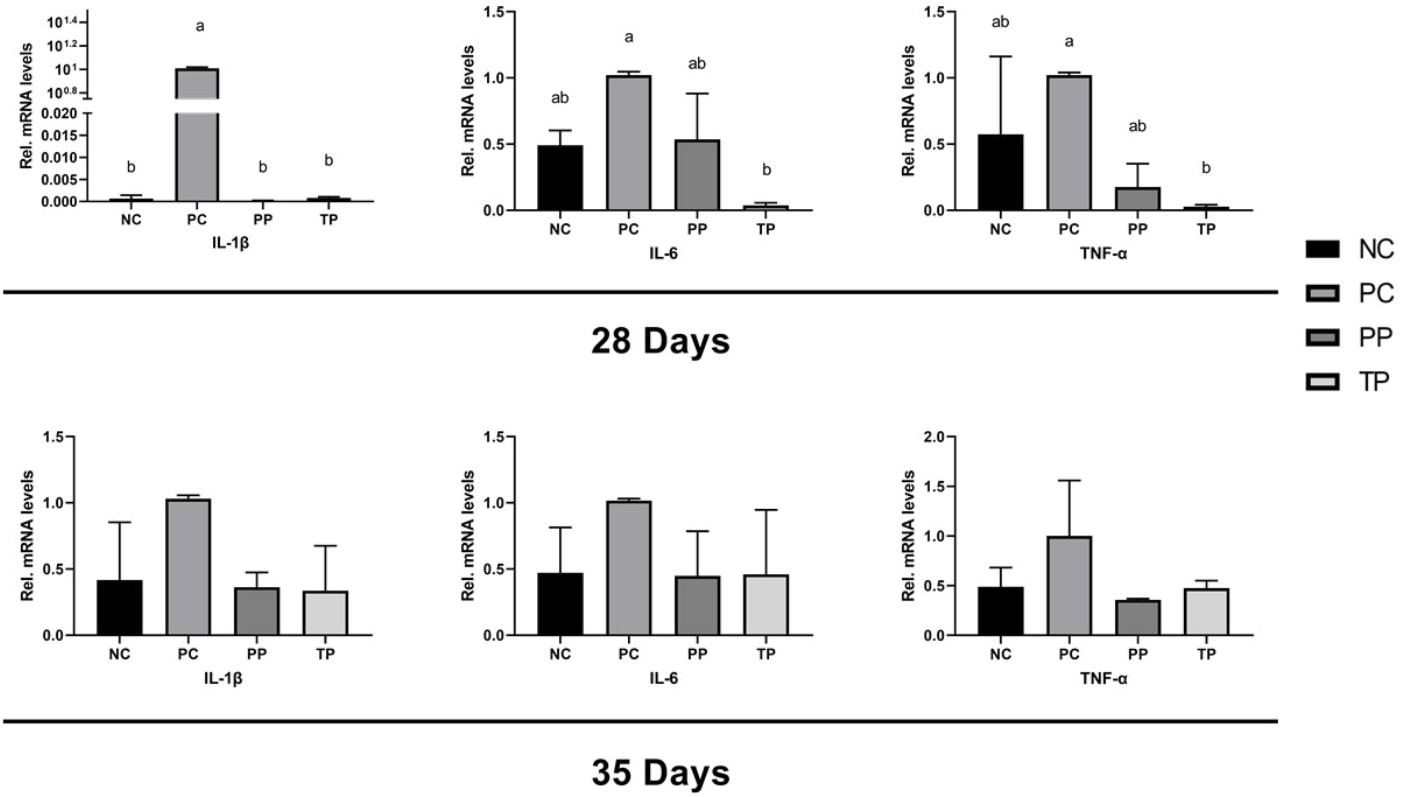

Figure 4 – Evaluation of ileal inflammation–associated gene expression in broiler samples collected at 28 and 35 days of age from four experimental groups: negative control (NC, basal diet), positive control (PC, basal diet + phospholipase C [PLC] challenge), prevention peptide (PP, basal diet + PLC challenge + 20 mg/kg antimicrobial peptide Q4-15-2A7P from days 1 to 35), and therapy peptide (TP, basal diet + PLC challenge + 20 mg/kg antimicrobial peptide Q4-15-2A7P from days 23 to 35). Data are presented as mean ± SD (n=3). [a-c] Mean values with different letters are significantly different ($p<0.05$). Abbreviations: IL-1β, interleukin 1β; IL-6, interleukin 6; TNF-α, tumor necrosis factor-α.

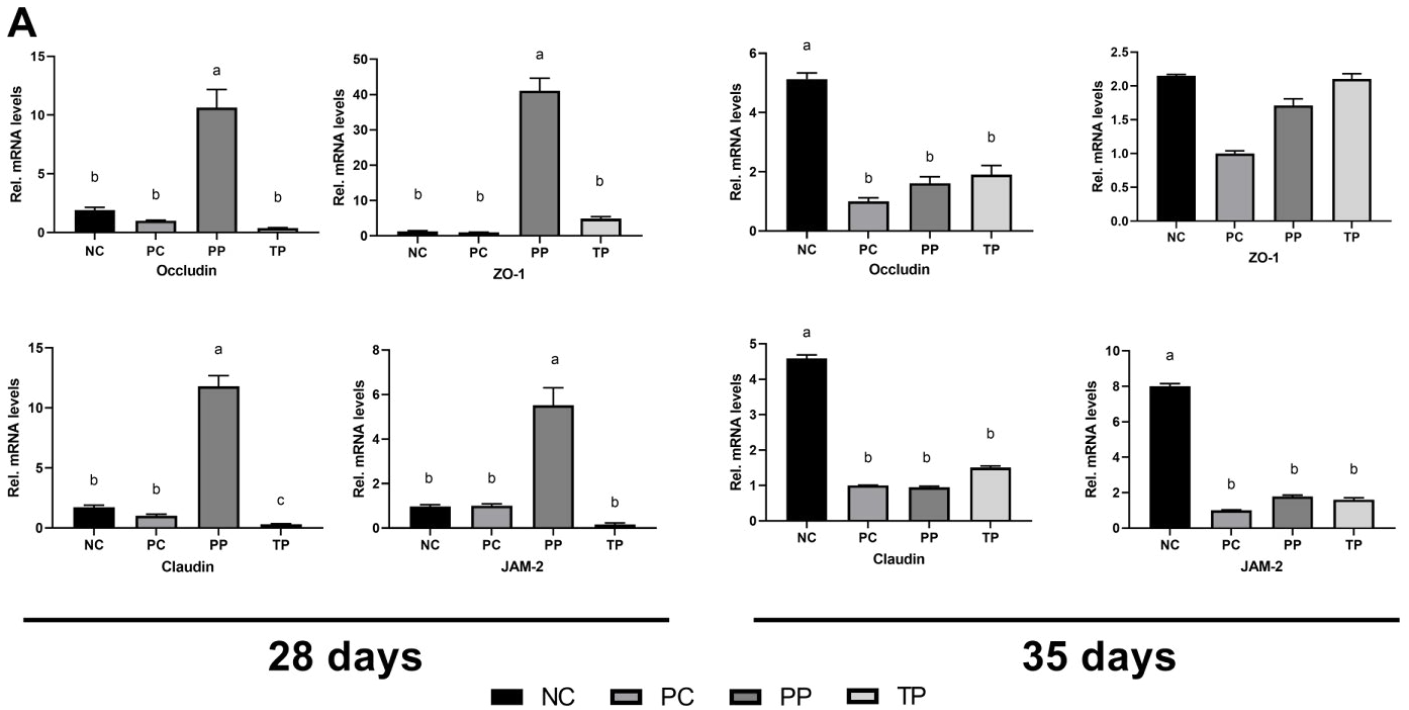

Figure 5 – Evaluation of ileal tight junction protein–associated gene expression in broiler samples collected at 28 and 35 days of age from four experimental groups: negative control (NC, basal diet), positive control (PC, basal diet + phospholipase C [PLC] challenge), prevention peptide (PP, basal diet + PLC challenge + 20 mg/kg antimicrobial peptide Q4-15-2A7P from days 1 to 35), and therapy peptide (TP, basal diet + PLC challenge + 20 mg/kg antimicrobial peptide Q4-15-2A7P from days 23 to 35). Data are presented as mean ± SD (n=3). [a-c] Mean values with different letters are significantly different ($p<0.05$). Abbreviations: JAM-2, Junctional adhesion molecule 2; ZO-1, zonula occludens-1.

Effect of Q4-15-2A7P on ileal microbiota of broilers

No significant between-group differences were identified in the microbial alpha-diversity indices (observed features, shannon, simpson, and chao1) in the ileal digesta of broilers (Figure 6). The effects of Q4-15-2A7P treatments on the beta-diversity and taxonomic composition of ileal microbiota are presented in Figure 7. The unweighted principal coordinate analysis (PCoA) revealed that the NC and TP groups formed tight and compact clusters, indicating strong internal consistency and minimal variance within these groups (Figure 7A). The PC group showed noticeable overlap with both NC and TP, suggesting a microbial composition partially resembling the unchallenged state, while the PP group exhibited distinct separation, reflecting a unique microbial profile influenced by prolonged Q4-15-2A7P supplementation. The weighted PCoA further highlighted tight clustering for the NC and TP groups (Figure 7B), with the PP group positioned distinctly at the upper side, indicating a shift in abundant taxa, while the PC group remained dispersed and non-overlapping with others. The principal component analysis (PCA) showed a tightly clustered NC group, while the PC, PP, and TP groups were more dispersed, with PP separating along the primary axis, suggesting a significant treatment effect on microbial structure (Figure 7C). The heatmap of top genera illustrated that PP and TP groups exhibited higher relative abundances of beneficial bacteria compared to PC, such as genus *Lactobacillus* (Figure 7D). The relative abundances of pathogens, such as genus *Escherichia-Shigella*, was lower in the PP and TP groups compared with the PC group (Figure 7D). The effects of Q4-15-2A7P treatments on bacterial taxonomy in the ileal microbiota of broilers are summarized in Table 7. No significant between-group differences were identified in the relative abundance of bacteria at the phylum, class, and order level. At the family level, the abundance of the family Enterobacteriaceae was significantly higher in the PC group compared with the TP group (p=0.03). There was no significant difference observed between the treatment groups in the relative abundance of bacteria at the genus level.

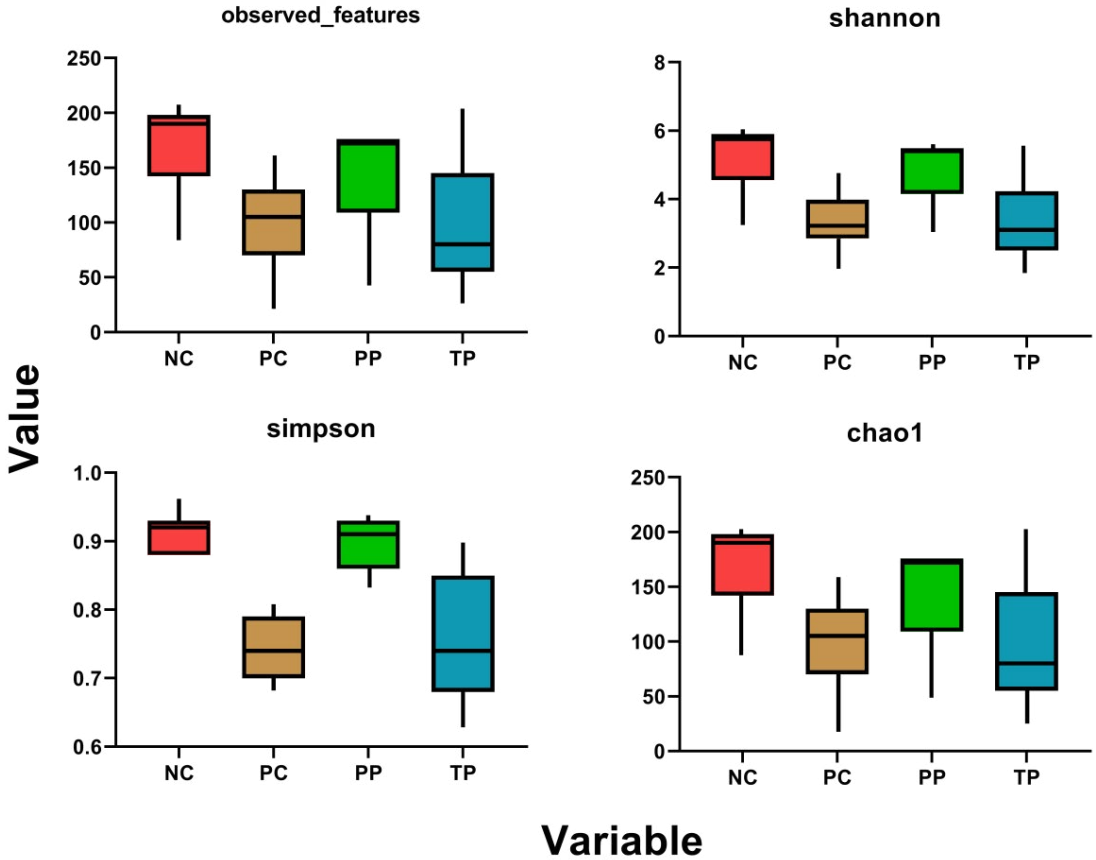

Figure 6 – Alpha-diversity indices of ileal microbiota in broiler samples collected at 35 days of age. Diversity metrics were assessed for four experimental groups: negative control (NC, basal diet), positive control (PC, basal diet + phospholipase C [PLC] challenge), prevention peptide (PP, basal diet + PLC challenge + 20 mg/kg Q4-15-2A7P from days 1 to 35), and therapy peptide (TP, basal diet + PLC challenge + 20 mg/kg Q4-15-2A7P from days 23 to 35). (A) Observed features index. (B) Shannon index. (C) Simpson index. (D) Chao 1 index. Three replicates were conducted for the analysis (n=3).

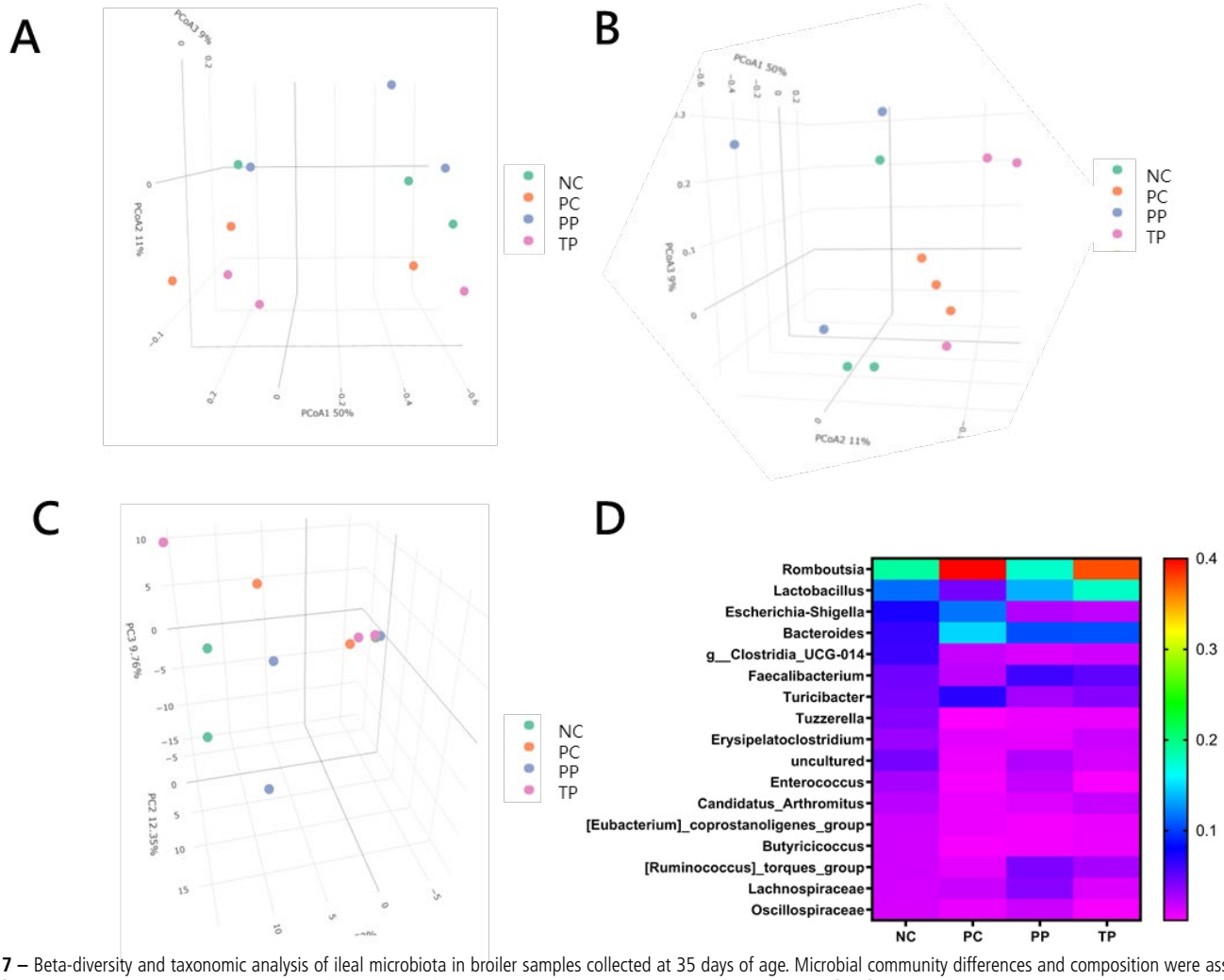

Figure 7 – Beta-diversity and taxonomic analysis of ileal microbiota in broiler samples collected at 35 days of age. Microbial community differences and composition were assessed among four experimental groups: negative control (NC, basal diet), positive control (PC, basal diet + phospholipase C [PLC] challenge), prevention peptide (PP, basal diet + PLC challenge + 20 mg/kg Q4-15-2A7P from days 1 to 35), and therapy peptide (TP, basal diet + PLC challenge + 20 mg/kg Q4-15-2A7P from days 23 to 35). (A) Unweighted principal coordinate analysis (PCoA). (B) Weighted principal coordinate analysis (PCoA). (C) Principal component analysis (PCA). (D) Heatmap of relative abundance of top genera. Three replicates were conducted for the analysis (n=3).

Table 7 – Effect of the antimicrobial peptide Q4-15-2A7P on the relative abundance in the ileal microbiota of broilers. (to be continue)

	Relative abundance (%)					
	NC[1]	PC	PP	TP	SEM	*p*-value
Phylum						
Firmicutes	85.9[2]	73.3	86.7	87.2	7.17	0.06
Bacteroidetes	6.4	14.9	10.8	10.7	3.58	0.08
Proteobacteria	7.7	11.7	2.5	2.1	3.52	0.05
Class						
Clostridia	60.6	60.0	60.3	62.2	0.96	0.50
Bacilli	25.3	13.3	26.4	25.0	3.66	0.07
Bacteroidia	6.4	14.9	10.8	10.7	3.59	0.07
Gammaproteobacteria	7.7	11.7	2.5	2.1	5.15	0.05
Order						
Peptostreptococcales-Tissierellales	20.1	43.5	19.7	39.4	5.89	0.05
Lachnospirales	13.3	5.7	19.5	7.9	5.19	0.05
Oscillospirales	20.5	7.32	16.9	12.0	5.55	0.05
Bacteroidales	6.9	15.5	13.7	11.5	3.98	0.06
Erysipelotrichales	9.5	8.8	4.9	6.5	1.47	0.32
Clostridiales	6.7	2.0	1.5	1.7	3.04	0.10

Table 7 – Effect of the antimicrobial peptide Q4-15-2A7P on the relative abundance in the ileal microbiota of broilers. (continued)

	Relative abundance (%)					
	NC[1]	PC	PP	TP	SEM	*p*-value
Family						
Lachnospiraceae	15.8	6.2	21.8	9.7	1.99	0.21
Bacteroidaceae	8.1	17.2	15.5	13.5	4.43	0.05
Ruminococcaceae	12.8	4.1	11.5	8.2	6.42	0.05
Enterobacteriaceae	8.4[ab]	12.1[a]	2.9[ab]	2.2[b]	5.39	0.03
Erysipelotrichaceae	7.0	7.7	4.5	4.7	0.47	0.78
Enterococcaceae	3.0	0.4	2.2	0.3	1.51	0.31
Genus						
Bacteroides	16.4	24.4	29.0	25.3	6.95	0.05
Lactobacillus	15.4	5.3	26.5	20.1	2.59	0.13
Romboutsia	28.5	44.3	28.5	40.8	2.33	0.17
Escherichia–Shigella	12.8	13.2	3.0	2.8	4.77	0.05
Turicibacter	11.6	7.7	5.2	5.1	0.40	0.83

[1] NC, basal diet; PC, basal diet plus 150 U PLC/day; PP, basal diet plus 150 U PLC/day and 20 mg/kg peptide Q4-15-2A7P from 1 to 35 days; TP, basal diet plus 150 U PLC/day and 20 mg/kg peptide Q4-15-2A7P from 23 to 35 days. [2] Mean values represent results from 3 replicate cages per treatment (n=3). [a-b] Mean values in the row with different superscripted letters are significantly different ($p<0.05$)

DISCUSSION

The application of PLC in this study was intended to mimic *C. perfringens*-mediated subclinical NE in broilers without inducing mortality. Intraperitoneal injection of PLC has been demonstrated to reduce body weight gain, compromise immune function, and diminish antioxidant capacity and intestinal health (Zhang *et al.*, 2024). The findings of this study underscore the efficacy of PLC as a nonlethal method for mimicking the pathological effects of *C. perfringens*, as evidenced by the significant reduction in daily feed intake and severe intestinal lesions in the PC group at both 28 and 35 days of age. This confirms the effectiveness of the *C. perfringens* toxin challenge model employed in the present study.

PLC, the enzymatic moiety of *C. perfringens* alpha-toxin, plays a central role in mediating intestinal damage during NE. Its zinc-dependent structure confers remarkable stability under the harsh conditions of the gastrointestinal tract, enabling it to resist proteolytic degradation and acidic environments (Monturiol-Gross *et al.*, 2014; Monturiol-Gross *et al.*, 2021; Coursodon *et al.*, 2010; Zhang *et al.*, 2024). This stability allows PLC to persist and continuously hydrolyze membrane phospholipids, thereby disrupting epithelial cell integrity and triggering cascades of inflammation and oxidative stress, as observed in the PC group's elevated ileal lesion scores compared to the NC group. The persistent activity of PLC not only facilitates bacterial translocation across compromised mucosal barriers but also amplifies host inflammatory responses, ultimately contributing to the pathogenesis of necrotic enteritis (Wade *et al.*, 2020; Zhang *et al.*, 2024). Therefore, alleviating PLC-mediated intestinal damage, as demonstrated by the PP and TP groups, could be a critical target for both the prevention and treatment of NE.

This study was designed to specifically investigate the potential of Q4-15-2A7P as a standalone AMP solution for managing *C. perfringens*-induced NE in broilers, with a particular emphasis on its dual role as a preventive and therapeutic agent. By limiting the experimental groups to NC, PC, PP, and TP, we isolated the effects of Q4-15-2A7P in both preventive and therapeutic contexts under a controlled PLC challenge. This streamlined approach allowed for a detailed assessment of its mechanisms—namely, its antimicrobial activity against *C. perfringens* and its anti-inflammatory properties—without the confounding variables introduced by additional comparators such as conventional antibiotics. While traditional antibiotics like enramycin have been widely studied (Muneeb *et al.*, 2025), their mechanisms are well-documented, and our focus was to explore a novel AMP as a next-generation alternative in the context of rising AMR, with a special interest in its potential as a prophylactic health supplement.

Consistent with a previous study (Yamawaki *et al.*, 2017), at 28 days of age, the PC group exhibited clear pathological changes induced by PLC, including hemorrhagic swelling and yellow-white diffuse lesions across all intestinal segments, compromising villus absorptive capacity and facilitating microbial translocation. This was reflected in the significantly reduced ADI in the PC group compared with the NC, PP, and TP groups, highlighting the adverse impact of PLC on appetite and activity. Intestinal lesion scores revealed more pronounced damage in the anterior intestine than in the middle and posterior sections, with PP showing a numerical reduction compared to PC, though not statistically significant, suggesting a potential early protective trend. Similarly, jejunal lesions in PP trended lower than PC, supporting a subtle mitigating effect. By 35 days of age, the PC group's intestinal damage persisted, whereas the PP and TP groups recovered to levels comparable to the NC group. Notably, the PP group consistently showed superior outcomes, such as higher duodenal villus height and lower inflammation at 28 days, suggesting that early and continuous administration of Q4-15-2A7P provides a proactive protective effect against PLC-induced pathology, potentially amplified by these early trends.

Although this study did not directly compare Q4-15-2A7P with conventional antibiotics, its efficacy can be contextualized against literature benchmarks. For instance, antibiotics like enramycin reduce *C. perfringens* proliferation by inhibiting cell wall synthesis (Muneeb *et al.*, 2025), yet their limited capacity to mitigate PLC-mediated damage has been noted (Wang *et al.*, 2023). In contrast, Q4-15-2A7P normalized feed intake by 1–27 days and reduced ileal lesion scores to NC levels by 35 days, while enhancing tight-junction protein expression (e.g., occludin and claudin in PP) and promoting a healthier microbial profile (e.g., increased genus *Lactobacillus* abundance). This multifaceted approach—combining antimicrobial action with anti-inflammatory and gut barrier-enhancing effects—positions Q4-15-2A7P as a superior alternative, particularly as a preventive strategy

where it preemptively limits damage compared to the reactive TP intervention.

The improvements in intestinal morphology and lesion scores attributed to Q4-15-2A7P are explained by its dual antimicrobial and anti-inflammatory properties. Similar to other synthetic AMPs, Q4-15-2A7P targets *C. perfringens* by disrupting bacterial cell membranes, reducing pathogen load and subsequent inflammation, as evidenced by lower IL-1β, IL-6, and TNF-α mRNA levels in PP and TP compared to PC at 28 days. Its anti-inflammatory effects mitigate PLC-triggered cascades (Monturiol-Gross *et al.*, 2014), preserving intestinal structure, as seen in the PP group's higher duodenal VH and VH:CD ratio at 28 days. Notably, PP also exhibited trends toward improved jejunal VH and ileum VH:CD at 28 days, suggesting a broader protective tendency not fully captured by statistical significance. At 35 days, the PP group's elevated VH:CD ratio and higher jejunal VH further reinforce this trend. The PP group's superior recovery, including the highest occludin and claudin expression at 28 days, with ZO-1 showing a non-significant but positive trend in PP and TP, underscores the advantage of early administration, establishing a protective barrier against PLC damage more effectively than the TP group's post-challenge intervention.

Q4-15-2A7P exhibits broad-spectrum antibacterial activity (Chou *et al.*, 2008), and we hypothesize that its ingestion modulates gut microbiota to favor beneficial species while suppressing potential pathogens. In this study, PP and TP groups showed a trend toward increased genus *Lactobacillus* abundance compared to PC, with PP exhibiting the highest levels, suggesting a stronger beneficial shift with prolonged administration. *Lactobacillus* species, known for enhancing nutrient absorption and gut barrier function (Kalavathy *et al.*, 2003; Singh *et al.*, 2012), likely contributed to the improved intestinal health in PP group in the present study. The unweighted PCoA revealed a clear separation of the PP group from NC, PC, and TP, reflecting a unique microbial community structure, while the weighted PCoA underscored PP's divergence in dominant taxa abundance, such as genus *Lactobacillus*. The heatmap of top genera further confirmed PP's distinct microbial profile, with elevated abundances of the genus *Lactobacillus* compared to PC, aligning with its beta-diversity separation. Conversely, Enterobacteriaceae abundance, linked to potential pathogenicity, was significantly reduced in TP compared to PC, with PP also trending lower than NC, reinforcing Q4-15-2A7P's selective suppression of harmful taxa. Unlike antibiotics that disrupt microbiota broadly, Q4-15-2A7P's selective action supports a resilient gut ecosystem, with PP's continuous supplementation maximizing these beneficial trends over TP's shorter intervention, as evidenced by its distinct clustering in PCA.

Q4-15-2A7P normalized ADI in PP and TP by 1–27 days. At 35 days, TP effectively reduced jejunal lesion scores to normal levels, indicating strong therapeutic efficacy, while both PP and TP normalized ileal lesions. However, PP's broader improvements across morphology and gene expression suggest that preventive use offers greater overall protection, supporting its potential as a health-promoting feed additive.

An interesting finding that warrants discussion is the observation at day 35, where despite morphological recovery, the expression of tight-junction-associated genes (occludin and claudin) in the PP and TP groups was lower than in the NC group. A possible explanation is that it is not a sign of functional failure but rather reflects a dynamic, two-phase repair process. At day 28, the upregulation of these genes, particularly in the PP group, likely represented a compensatory repair mechanism initiated in response to the PLC-induced barrier disruption. Once intestinal integrity was largely re-stored by day 35, as evidenced by the improved lesion scores, the potent stimulus for this "emergency" gene expression was consequently removed. The system then returned from a state of high-intensity repair to a new homeostatic level. This new state might be lower than the baseline of the NC group, potentially reflecting a quiescent phase to conserve energy after a major repair event, in contrast to the continuous maintenance in the un-challenged gut. This phenomenon of transient gene upregulation during tissue injury followed by a return to homeostasis is well-documented in various biological models of epithelial repair (Groschwitz and Hogan, 2009; Turner, 2009).

A limitation of this study is the lack of direct antibiotic comparison, though the well-documented resistance and limited anti-inflammatory effects of agents like enramycin (Belote *et al.*, 2018) bolster Q4-15-2A7P's case as a standalone candidate. Enramycin is highly effective in controlling necrotic enteritis caused by *Clostridium perfringens* through its anti-bacterial activity. However, there are no relevant findings to demonstrate that enramycin is able to alleviate PLC-induced necrotizing enteritis through either direct or indirect interaction. Future studies should test it against probiotics or other AMPs, and under direct *C.*

perfringens challenge to confirm its preventive efficacy in real-world settings.

These findings have significant practical implications for the poultry industry, particularly in the context of "antibiotic-free" production systems. The promise of Q4-15-2A7P as a prophylactic feed additive, however, hinges on its economic feasibility. The primary obstacle to the widespread adoption of AMPs in commercial settings is their high production cost compared to conventional antibiotics. For Q4-15-2A7P to be viable for production-scale implementation, future research must focus on developing cost-effective, large-scale synthesis methods. This could involve optimizing solid-phase synthesis or exploring recombinant expression system using microbial hosts in the future.

CONCLUSION

Preventive and therapeutic administration of Q4-15-2A7P enhanced average daily feed intake, reduced intestinal lesion scores, improved gut morphology, and modulated intestinal gene expression and microbiota composition in broilers under *C. perfringens* toxin challenge. The PP group's superior outcomes highlight its potential as a prophylactic feed supplement, effectively supporting gut integrity, reducing inflammation, and promoting microbial balance, offering a sustainable alternative to antibiotics without dysbiosis risks. Further validation under direct bacterial challenge is needed to solidify its adoption in poultry production.

ACKNOWLEDGEMENTS

None.

AUTHOR CONTRIBUTIONS

Conceptualization, Yu YH, and Chen WJ; methodology, Cheng YH, Yu YH, and Chen WJ; validation, Horng YB, Cheng YH; formal analysis, Horng YB, Cheng YH; investigation, Horng YB, Cheng YH, Yu YH, and Chen WJ; resources, Cheng YH and Chen WJ; data curation, Horng YB and Cheng YH; writing—original draft preparation, Horng YB; writing—review and editing, Yu YH and Chen WJ; supervision, Yu YH and Chen WJ; project administration, Yu YH and Chen WJ; funding acquisition, Chen WJ. All authors have read and agreed to the published version of the manuscript.

FUNDING

This work was supported by the National Science and Technology Council (NSTC 111-2313-B-197-004-MY3) in Taiwan.

DATA AVAILABILITY STATEMENT

The data that support the findings of this study are available upon reasonable request.

CONFLICT OF INTEREST

The authors declare no conflict of interest.

REFERENCES

Belote BL, Tujimoto-Silva A, Hümmelgen PH, *et al.* Histological parameters to evaluate intestinal health on broilers challenged with *Eimeria* and *Clostridium perfringens* with or without enramycin as growth promoter. Poultry Science 2018;97:2287-94. https://doi.org/10.3382/ps/pey064

Boodhoo N, St-Denis M, Zheng J, *et al. In vivo* overexpression of the avian interleukin-17 in a necrotic enteritis disease model modulates the expression of antimicrobial peptides in the small intestine of broilers. Cytokine 2024;183:156749. https://doi.org/10.1016/j.cyto.2024.156749

Cheng YH, Zhang N, Han JC, *et al.* Optimization of surfactin production from *Bacillus subtilis* in fermentation and its effects on *Clostridium perfringens*-induced necrotic enteritis and growth performance in broilers. Journal of Animal Physiology and Animal Nutrition 2018;102:1232-44. https://doi.org/10.1111/jpn.12937

Chou HT, Kuo TY, Chiang JC. Design and synthesis of cationic antimicrobial peptides with improved activity and selectivity against *Vibrio* spp. International Journal of Antimicrobial Agents 2008;32:130-138. https://doi.org/10.1016/j.ijantimicag.2008.04.003

Chou HT, Wen HW, Kuo TY, Lin CC, Chen WJ. Interaction of cationic antimicrobial peptides with phospholipid vesicles and their antibacterial activity. Peptides 2010;31:1811-20. https://doi.org/10.1016/j.peptides.2010.06.021

Coursodon CF, Trinh HT, Mallozzi M, *et al. Clostridium perfringens* alpha toxin is produced in the intestines of broiler chicks inoculated with an alpha toxin mutant. Anaerobe 2010;16:614-7. https://doi.org/10.1016/j.anaerobe.2010.09.006

Fathima S, Hakeem WGA, Shanmugasundaram R, *et al.* Necrotic enteritis in broiler chickens: a review on the pathogen, pathogenesis, and prevention. Microorganisms 2022;10:1958. https://doi.org/10.3390/microorganisms10101958

Fatmawati NND, Sakaguchi Y, Suzuki T, *et al.* Phospholipase C produced by *Clostridium botulinum* types C and D: comparison of gene, enzymatic, and biological activities with those of *Clostridium perfringens* alpha-toxin. Acta Medica Okayama 2013;67:9-18. https://doi.org/10.18926/AMO/49252

Fodor A, Vellai T, Hess C, *et al.* XENOFOOD—an autoclaved feed supplement containing autoclavable antimicrobial peptides—exerts anticoccidial GI activity, and causes bursa enlargement, but has no detectable harmful effects in broiler cockerels despite *in vitro* detectable cytotoxicity

on LHM cells. Pathogens 2023;12:458. https://doi.org/10.3390/pathogens12030458

Groschwitz KR, Hogan SP. Intestinal barrier function: molecular regulation and disease pathogenesis. Journal of Allergy and Clinical Immunology 2009;124:3-20; https://doi.org/10.1016/j.jaci.2009.05.038

Kalavathy R, Abdullah N, Jalaludin S. Effects of *Lactobacillus* cultures on growth performance, abdominal fat deposition, serum lipids and weight of organs of broiler chickens. British Poultry Science 2003;44:139-44. https://doi.org/10.1080/0007166031000085445

Kim SJ, Kang TB, Kim DH, *et al.* 10-mer and 9-mer WALK peptides with both antibacterial and anti-inflammatory activities. Antibiotics 2022;11:1588. https://doi.org/10.3390/antibiotics11111588

Kiu R, Hall LJ. An update on the human and animal enteric pathogen *Clostridium perfringens*. Emerging Microbes & Infections 2018;7:141. https://doi.org/10.1038/s41426-018-0144-8

Liang Q, Cao L, Zhu, C, *et al.* Characterization of recombinant antimicrobial peptide BMGlv2 heterologously expressed in *Trichoderma reesei*. International Journal of Molecular Sciences 2022;23:10291. https://doi.org/10.3390/ijms231810291

Meogrossi G, Tollapi E, Rencinai A, *et al.* Antibacterial and anti-inflammatory activity of branched peptides derived from natural host defense sequences. Journal of Medicinal Chemistry 2024;67:16145-56. https://doi.org/10.1021/acs.jmedchem.4c00810

Möllby R, Wadström T. Purification of phospholipase C (alpha-toxin) from *Clostridium perfringens*. Biochimica et Biophysica Acta 1973;321:569-84. https://doi.org/10.1016/0005-2744(73)90200-3

Monturiol-Gross L, Flores-Díaz M, Pineda-Padilla MJ, *et al. Clostridium perfringens* phospholipase C induced ROS production and cytotoxicity require PKC, MEK1 and NFκB activation. PLoS ONE 2014;9:e86475. https://doi.org/10.1371/journal.pone.0086475

Monturiol-Gross L, Villalta-Romero F, Flores-Díaz M. Bacterial phospholipases C with dual activity: phosphatidylcholinesterase and sphingomyelinase. FEBS Open Bio 2021;11:3262-75. https://doi.org/10.1002/2211-5463.13320

Muneeb M, Khan EU, Ali M, *et al.* Effects of replacing antibiotics with probiotics and antimicrobial peptides on performance, gut health, carcass traits, meat quality, and welfare in broilers infected with *Eimeria* and *Clostridium perfringens*. Tropical Animal Health and Production 2025;57:184. https://doi.org/10.1007/s11250-025-04441-4

Rautenschlein S, Kraemer C, Vanmarcke J. Protective efficacy of intermediate and intermediate plus infectious bursal disease virus (IBDV) vaccines against very virulent IBDV in commercial broilers. Avian Diseases 2005;49:231-7. https://doi.org/10.1637/7310-112204R

Singh KM, Shah T, Deshpande S, *et al.* High through put 16S rRNA gene-based pyrosequencing analysis of the fecal microbiota of high FCR and low FCR broiler growers. Molecular Biology Reports 2012;39:10595-602. https://doi.org/10.1007/s11033-012-1947-7

Son H, Park SC, Kim YM, *et al.* Potent anti-inflammatory effects of a helix-to-helix peptide against *Pseudomonas aeruginosa* endotoxin-mediated sepsis. Antibiotics 2022;11:1675. https://doi.org/10.3390/antibiotics11111675

Turner JR. Intestinal mucosal barrier function in health and disease. Nature Reviews Immunology 2009;9:799-809. https://doi.org/10.1038/nri2653

Wang S, Zeng X, Yang Q, Qiao S. Antimicrobial peptides as potential alternatives to antibiotics in food animal industry. International Journal of Molecular Sciences 2016;17:603. https://doi.org/10.3390/ijms17050603

Wang X, Zhang T, Li W, *et al.* Arginine alleviates *Clostridium perfringens* α toxin-induced intestinal injury *in vivo* and *in vitro* via the SLC38A9/mTORC1 pathway. Frontiers in Immunology 2024;15:1357072. https://doi.org/10.3389/fimmu.2024.1357072

Wang Y, Li J, Dai X, *et al.* Effects of antimicrobial peptides Gal-13 on the growth performance, intestinal microbiota, digestive enzyme activities, intestinal morphology, antioxidative activities, and immunity of broilers. Probiotics and Antimicrobial Proteins 2023;15:694-705. https://doi.org/10.1007/s12602-021-09905-1

Wade B, Keyburn AL, Haring V, *et al.* Two putative zinc metalloproteases contribute to the virulence of *Clostridium perfringens* strains that cause avian necrotic enteritis. Journal of Veterinary Diagnostic Investigation 2020;32:259-67. https://doi.org/10.1177/1040638719898689

Wu KC, Hua KF, Yu YH, *et al.* Antibacterial and antibiofilm activities of novel antimicrobial peptides against multidrug-resistant enterotoxigenic *Escherichia coli*. International Journal of Molecular Sciences 2021;22:3926. https://doi.org/10.3390/ijms22083926

Yeaman MR, Yount NY. Mechanisms of antimicrobial peptide action and resistance. Pharmacological Reviews 2003;55:27-55. https://doi.org/10.1124/pr.55.1.2

Yamawaki Y, Oue K, Shirawachi S, *et al.* Phospholipase C-related catalytically inactive protein can regulate obesity, a state of peripheral inflammation. Japanese Dental Science Review 2017;53:18-24. https://doi.org/10.1016/j.jdsr.2016.06.001

Zhang T, Wang X, Li W, *et al. Clostridium perfringens* α toxin damages the immune function, antioxidant capacity and intestinal health and induces PLCγ1/AMPK/mTOR pathway-mediated autophagy in broiler chickens. Heliyon 2024;10:e26114. https://doi.org/10.1016/j.heliyon.2024.e2611485

DISCLAIMER/PUBLISHER'S NOTE